

# Revealing Rheological Parameters of Cotton-stitch-modified Cotton Fabrics by Three-Network Modeling (TNM) of Materials

Harmony Werth<sup>1, #</sup>, Kazi Zihan Hossain<sup>1, #</sup>, M. Rashed Khan<sup>1, \*</sup>

<sup>1</sup>Department of Chemical and Materials Engineering, University of Nevada, Reno

#contributed equally

\*Corresponding author: mrkhan@unr.edu

## Abstract

Cotton threads and fabrics are the most used textile materials and have garnered widespread interest for smart textiles to capture human-centered cyber-physical and human-health-related bioanalytical data. Cotton threads are sewn (manually or digitally) into fabrics to achieve functional and fashion stitches that soften or stiffen the base fabric. There has been limited investigation into the influence of a single stitch on the mechanical properties of knitted cotton fabric. Such understanding may become critical to producing optimized textile-based composites/smart materials involving sewing operations. While stitching operations are investigated in numerous ways to produce a range of smart wearables, herein, we demonstrate the rheological modification of base cotton fabric induced by two types of singular stitches (straight and zigzag). We have sewn simple straight and zigzag cotton stitches to investigate the rheological modification of the base cotton fabrics. Uniaxial stress-strain experimental data, combined with constitutive modeling (i.e., three-network model, TNM) obtained from the calibration software (MCalibration), revealed the feasibility of a data-driven approach to investigate the rheological parameters. Our experimental analyses, combined with the calibrated data, suggest a 99.99% confidence in assessing the influence of a single stitch on knitted cotton fabrics. We have also used distributed strain energy to analyze the mechanics and failure of the base and stitched fabrics. Our study may enable the design and study of integrating smart threads in cotton fabrics to produce smart wearables, e-textile, biomedical and e-fashion textiles.

## Introduction

Knitted cotton fabrics have been utilized in everyday garment materials and emerged as one of the popular base materials to generate smart wearables. In this article, we reveal rheological parameters- also known as phenomenological parameters, of cotton-stitch-modified cotton fabrics, harnessing Three Network Models (TNM).<sup>1,2</sup> We produce two types of stitches for demonstrations to modify the mechanical behavior of knitted cotton fabrics. While the utility of cotton fabrics is ubiquitous, and numerous demonstrations are currently published in the literature, our study focuses on understanding the tuned mechanics of cotton fabrics by sewn stitches and unravels data that we often overlook through stress-strain analyses. Anisotropy of knitted cotton fabric and its modified structural properties exhibited deformations during mechanical performance analyses.<sup>3</sup> Several studies focused on understanding knit fabrics, fabric elongation, deformation, and failures at critical applied stress.<sup>4-10</sup> Advanced applications on knitted fabrics are approached mainly by trial and error methods where in-plane stitches are randomly generated, leaving a knowledge gap in understanding the impact of final sewn stitches on fabrics. Sewing- one of the ancient fabric manufacturing techniques, loops a thread into fabrics, leveraging an analog or computerized sewing machine. Different sewing stages,<sup>11</sup> sewing parameters,<sup>12</sup> and sewing machines<sup>13,14</sup> have also been reported to alter the properties of the sewing thread. The looping process integrates different threads and produces entanglements with aesthetic colors, body shapes, and on-demand geometries. Different stitch patterns have also been reported to change the rheological behavior of the sewing thread.<sup>15,16</sup> However, the rheological impact on the fabric due to stitching has not been adequately investigated. While the original purpose of sewing has been joining two pieces of fabric together, the most advanced applications integrate smart threads so that biomedical, biochemical, and biological analyses can be performed *in situ*.<sup>17,18</sup> From the design of fashion to human-centered smart wearables, state-of-sewing leverages many stitch patterns; however, a data-informed approach to dissect the role of sewn stitches in manipulating the final fabrics' properties is currently lacking in the literature.

Using a sewing machine, sewn stitches create entanglements between two threads- an upper and a bobbin thread, the bottom thread. During the entanglement, the sewing needle loops the upper thread between the bottom thread through the fabric, and the threads entangle. When the tension of both threads matches, the entanglement lays in-plane of the fabric on both sides with minimal damage.<sup>19</sup> The resulting stitch can be varied in numerous ways to create functional and non-functional patterns based on the types of sewing threads, fabric types, or choice of materials for the final composite structures.<sup>20</sup> Concurrently, stitches are used to bind two or more layers of fabric together, which is known as a seam. To determine the impact of stitches on the mechanical behavior of fabrics, a few research groups have tested seams in woven cotton fabric.<sup>21-23</sup> A few investigations on the mechanical behavior of seams in knitted fabrics are also available in the literature.<sup>24,25</sup> However, studies involving a single stitch thread to modify the mechanical behavior of cotton fabric are currently lacking for a single layer of fabric. Such studies, we believe, will become significantly crucial for future applications, i.e., electronic textiles- because reducing materials consumption at an optimum number of

trials and errors seems crucial to pursue robust design configurations during the development of smart threads and electronic fabrics.

The base fabric and thread used in this work are made from cotton. We assume both as an elastomeric network for modeling. Elastomers having 3,000 to 10,000 repeating units exhibit structural flexibility and experience stretch-induced softening/hardening (also known as Mullins damage) under applied loads.<sup>26</sup> For data calibration, we use TNM in MCalibration software which maps the entire stress-strain spectra from the uniaxial test. The TNM is also known as a phenomenological model to describe deformation-induced structural evolution (i.e., the transition between soft to stiff network) and how strain-energy density becomes redistributed (i.e., hysteresis) throughout the experiments. Different hyperelastic models have been utilized in the literature to represent the rheological behavior of fabrics.<sup>27–31</sup> However, according to our knowledge, this work presents the constitutive modeling of stitched fabrics with TNM for the first time. The data-calibration process in MCalibration can start using default or user-induced settings. For this study, we have chosen to start calibration using default settings in MCalibration. The kinematics of the TNM consists of three parallel molecular networks. We have assumed spring-dashpot domains connected in parallel for the first two, and the third one is only a spring depicting the hyperelasticity of the first two networks. The semi-crystalline domains are captured through the spring dashpots. While a single network can be used to evaluate the property of the entire composite structure, we have chosen TNM to capture effective viscoplasticity.<sup>1</sup>

Here, we have chosen two types of sewing stitches: straight and zigzag, to establish and reveal rheological parameters of cotton-stitch modified cotton fabrics, harnessing TNM. These stitches are common in sewn garments and are pre-programmed into the default settings of modern sewing machines. Also, we investigate several variations of the zigzag stitch that has varying stitch length and width. A commercial sewing machine creates stitches with 100% cotton materials (i.e., threads and fabrics). For our analyses, we investigate the surface topography of the fabric and samples with sewn stitches using optical and scanning electron microscope (SEM) images. We perform (a) uniaxial stress-strain and (b) repeated cyclic tests in an Instron to dissect the mechanical behaviors of the (a) base fabric, (b) base threads, and (c) threads-laid-fabric structures. The uniaxial stress-strain analyses have revealed three regions of interest (i.e., elastic, yield, and viscoplastic). Also, we have investigated the permanent failure of the entire composite (fracture) to find the extremities of experimental analyses. The cyclic tests provide information about hysteresis, which we leverage to understand distributed strain-energy density and the loss due to hysteresis. We outline calibration using TNM in MCalibration to provide a simple route to test the impact of specific sewing patterns on the mechanical behavior of the final fabric. We hypothesize that the thread, which has significantly denser strain energy, shifts the fabric's macroscale stress-strain behavior after stitching. We proved our hypothesis through the uniaxial test and then altered the stitch length to investigate the factors that cause specific changes in the stress-strain behavior. The understanding developed by investigating the changes in mechanical behavior can be used to optimize the mechanical properties of a composite made with cotton thread and fabric.

## Materials and Methods

Our experiments were performed to determine a constitutive equation to represent the behavior of cotton fabric with different types of stitches. This was accomplished by analyzing uniaxial stress-strain curves for each component (cotton fabric and cotton thread) and different variations of the overall composite (straight stitched fabric, zigzag stitch, and fabric with stitching holes but no thread).

### *Materials*

The fabric used in this experiment was 100% cotton jersey knit with a unit weight of 427 g/m<sup>2</sup> obtained from Hobby Lobby Stores, Inc. The measured thickness of the fabric was 0.45 mm. Similarly, the thread used in this experiment was a 50-weight, 4-ply, 100% cotton thread of Sew-Ology Brand from Hobby Lobby Stores, Inc., produced for machine quilting. The measured outer diameter of the thread was 0.30 mm. The same thread was used for the top and bobbin threads for all samples prepared and presented in this work.

### *Sample Preparation*

We used a Brother SE600 sewing machine from Amazon to create stitches of manually adjustable length and width. The tension was selected so that the tension on the bobbin thread and the upper thread were equal, preventing the bottom thread from showing on the top or vice-versa, as is common sewing practice. A swatch of fabric approximately 20 cm in length was cut with scissors and then sewn wale-wise with the appropriate type of stitch for the sample. Two samples were prepared with stitching: straight stitched and zigzag stitched. The straight stitch was 2 mm in length. The zigzag stitches were (listed as stitch length x stitch width): 2x5 mm, 1x5 mm, 3x5 mm, 2x3 mm, and 2x4 mm. Several samples without any sewn stitches were also prepared for comparison. The fabric samples were then cut to the same size with a Cricut Maker fabric cutter bought from Amazon, allowing for accurate and reproducible sample cutting. For every sample, the fabric was cut to the dimensions of 6 cm in length by 2 cm in width. Sample cutting was done carefully to keep the stitching in the center of the sample. Damaged or samples with uncentered stitches were discarded without any analysis.

### *Image Acquisition*

Olympus SZ61 Stereo-microscope loaded with an Amscope MU1000-HS camera was used to capture the optical microscopic images. Secondary electron images of the samples were captured using a Thermo Scientific Scios 2 SEM. For SEM imaging, small representative samples were cut and loaded on the sample holder with double-sided carbon tape. Attention was given to keeping the stitch undamaged while loading on the holder. Since the samples were nonconductive, samples were sputter-coated with Gold (Au) to create a ~10 nm layer on the surface of the sample before imaging. Further optical images were captured with the camera on an iPhone 13 mini.

### *Experimental Methods*

The data was collected using an Instron 5982 test machine for uniaxial tensile testing. The tested area was 4 cm by 2 cm. The extra centimeter on each side allowed the grip to hold the sample during testing. Each sample type was examined with tensile testing to determine the stress and strain until failure at a 40 mm/min strain rate. Cyclic testing of four cycles was then conducted for specific samples up to a sustainable strain level for that sample type. Samples with straight stitches could only withstand slightly more than 10% strain. Therefore, cyclic tests with straight stitches were conducted up to 10% strain. For comparison, cyclic testing up to 10% strain was also conducted for unaltered fabric samples and the 2x5 mm zigzag stitch.

### *Strain-energy Density Calculation*

Using the trapezoidal rule, we calculated strain-energy density from the time-dependent force and stress data at varying strain rates. The area under the stress-strain or force-strain curve is divided into equal-time steps. Each small area under the curve is added until we reach the last data point to get the total area under the curve. The reported energy density from different observations is the total after each experimental stress-strain observation.

### *Constitutive Modeling of Different Fabrics*

An initial prediction of the strain energy density of the straight stitched sample was obtained based on the data collected from the unaltered fabric and thread samples. In order to obtain the prediction, the strain energy density of the straight stitch sample and the unaltered fabric was obtained by finding the area under the stress-strain curve of the sample with the trapezoidal rule. The strain energy density was calculated up to 4.5% strain because the thread samples failed around 5% strain. The strain energy of the samples was calculated by multiplying the strain energy density by the volume of the sample. The volume of the fabric was calculated using the sample's length, width, and thickness. The thread volume was calculated from the measured diameter and length of the thread sample. The straight stitch sample can be approximated by one sample of fabric and two samples of thread, so the volume of the straight stitch sample was calculated by adding the volume of the unaltered fabric and two threads. Similarly, the predicted strain energy of the straight stitch sample was calculated by adding the strain energy of the unaltered fabric and two threads. The prediction for the strain energy density of the straight stitched sample could then be obtained by dividing the predicted stored energy by the calculated volume.

MCalibration, from PolymerFEM,<sup>32</sup> was used to obtain parameters for a material model capable of representing the mechanical behavior of the fabric samples prepared in this work. MCalibration fits the experimentally collected uniaxial stress-strain data to the PolyUMod Three Network model.<sup>2</sup> An average of the stress-strain behavior of each sample type was obtained first. This set of averaged data was then processed using the MCalibration software tools to prepare the data for calibration. The default settings were used for the calibration. The calibrated parameters were exported and analyzed after the automatic convergence of the calibration process.

## Results and Discussion

### Surface Topography

We formed two different types of stitches on the base fabric. Figures 1a and 1b are top-down optical microscope images of the base and sewn fabrics for visual inspection. Figure 1b is a zoomed-in visual inspection of Figure 1a to identify differences between a straight stitch and a zigzag stitch on the in-laid fabric. These images show that the straight and zigzag stitches went through the fabric without significant internal damage. The straight stitch shown in Figures 1a(ii) and 1b(ii) do not have significant bunching due to the stitch compared with the only fabric shown in Figures 1a(i) and 1b(i); However, a meandering network of the zigzag stitches caused the fabric within the stitch to significantly bunch together, as shown in Figures 1 a(iii) and 1b(iii). The fabric is unable to maintain its shape during sewing and is pulled into the stitch instead. The structural stiffness and flexibility of the fabric may have contributed to the bunching, as observed within the stitch dimensions. Figure 1c is the sewn fabric's SEM images to investigate the surface topography of the stitches and fabric. SEM images in Figure 1c(i) and Figure 1c(ii) reveal the undamaged fabric by fibers. From these visual inspections, we assume the fabric remains structurally robust during the sewing and stitches only alter the mechanical behavior.

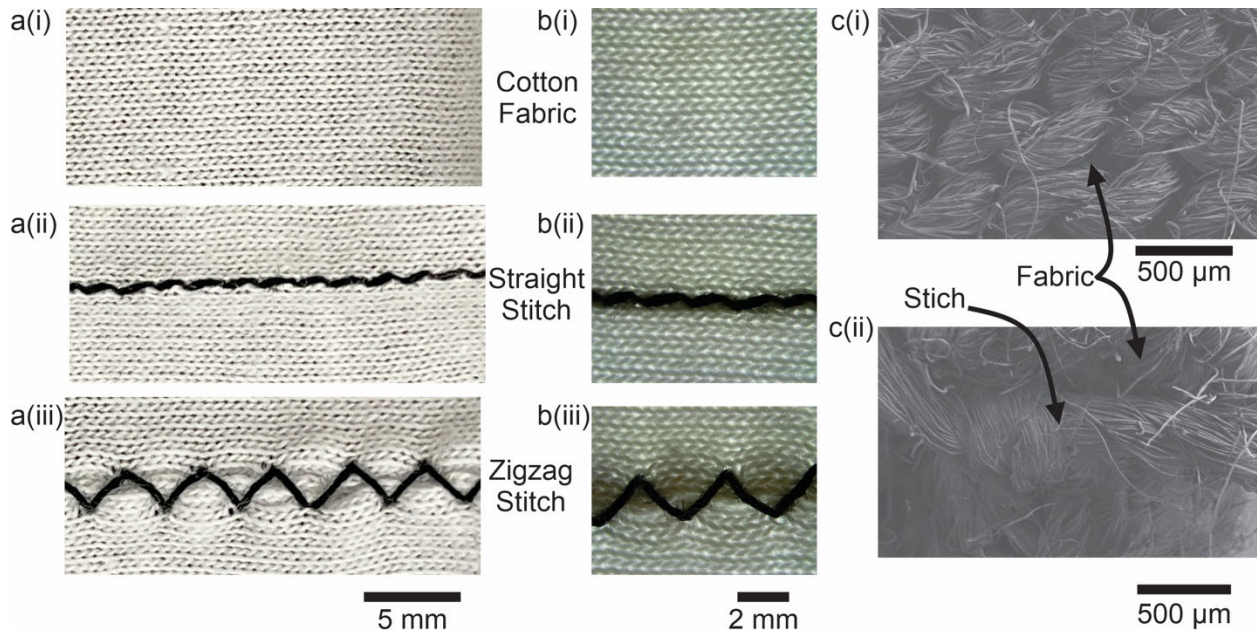


**Figure 1:** (a) Images were taken of samples under normal lighting conditions for visual inspection. (b) A stereoscope was used to examine the samples. (c) Secondary electron SEM images were taken of the fabric and sewn stitches.

### Uniaxial Tensile Behavior

We investigated plain thread, plain fabric, and stitched fabrics using Instron for mechanical behavior analyses. The uniaxial tensile test behavior of plain thread is shown

in Figure 2a, and the plain fabric is shown in Figure 2b. For comparison, Figure 2b also shows the behaviors of straight and zigzag (2x5mm) stitched fabrics. Four other zigzag stitched fabrics' behavior is shown in Figure 2c. Figures 2d and 2e show the side view of a zigzag stitched fabric loaded into Instron during tensile testing and at the end of failure analyses.

We tested two samples of the plain threads, and both samples' behavior is shown in Figure 2a. The plain thread failed at 5% strain but exhibited the highest strain energy density compared to other samples tested. In contrast to the plain thread, the cotton fabric in Figure 2b exhibited reproducible stretchability of up to 70% strain in two samples. The inclusion of straight stitches into the plain fabric induced failure at ~12% strain, and the zigzag stitched sample failed at ~32% strain.

The unaltered fabric had the highest strain at the point of failure, shown in Figure 2b, between 60-80%, with a strain energy density of around  $1.0 \text{ MJ/m}^3$  at failure. In comparison, the thread samples had a strain energy density of approximately  $5.0 \text{ MJ/m}^3$  at failure, which occurred at around 5% strain. The strain energy density of the unaltered fabric and thread at 4.5% were  $4.19 \times 10^{-4} \text{ MJ/m}^3$  and  $4.64 \text{ MJ/m}^3$ , respectively. Examining the stress-strain data for the cotton fabric and the cotton thread individually, we conclude that combining these materials would result in a sample with a strain energy density that falls between the different materials at a given strain. The samples with sewn straight stitches of 2mm length failed between 10-15% strain. At a strain of 4.5%, the straight stitched samples exhibited an average strain energy density of  $1.88 \times 10^{-3} \text{ MJ/m}^3$ . A prediction of the strain energy density of the straight stitched samples at 4.5% was obtained using the experimental values of the thread and fabric alone. The predicted value was  $7.2 \times 10^{-2} \text{ MJ/m}^3$ , more significant than the measured strain energy density. This discrepancy is expected as the sewing process exposes the thread to dynamic loads and friction known to reduce the strength of the thread.<sup>33</sup> Overall, the sample with sewn straight stitches failed at all fabric samples' lowest stress and strain. The cause of the low stress and strain at failure is suspected to be the structure of the stitches, which cannot withstand as much strain as the fabric. The fabric, with a higher elongation at failure than the thread, can deform under the load. Therefore, the thread in the straight stitch withstands the load for the entire sample until the thread breaks, equivalent to sample failure. It was observed that the thread failed before the fabric in all samples with straight stitches.

Samples with zigzag stitches of 2mm length and 5mm width also failed at stress and strain lower than the unaltered fabric but higher strain than the straight stitched sample. An analysis of the strain energy density of the 2x5mm zigzag sample reveals aspects of the mechanical behavior. At strains below 20%, the strain energy density of the 2x5mm zigzag sample is indistinguishable from the strain energy density of the fabric; Therefore, the fabric's mechanical properties dominate the thread's properties in the 2x5mm zigzag sample at strains under 20%. At 30% strain, the strain energy density of the zigzag sample is nearly double that of the fabric sample. The departure of the 2x5mm zigzag sample from the mechanical behavior of the fabric indicates that at strains above 20%, the thread is the dominant influence on the mechanical behavior. This behavior is

investigated further in zigzag samples with varying stitch lengths and widths, as indicated in Figure 2c.

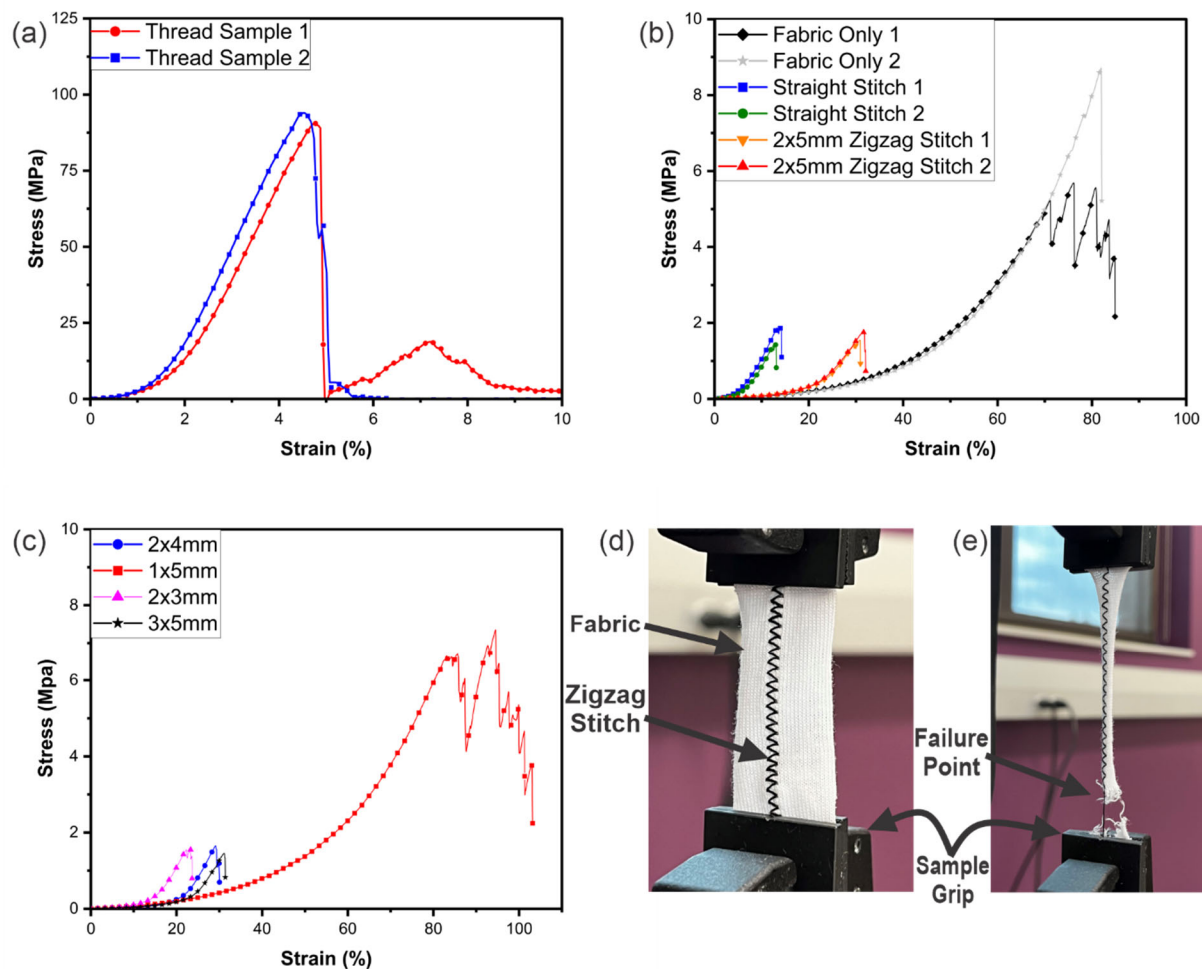


**Figure 2:** (a) The graph of the stress-strain curve for the samples of the cotton thread indicates maximum stress of approximately 100MPa at a strain of approximately 4.5% before failure. (b) The graph shows the stress-strain curves of the unaltered fabric, fabric with straight stitches of 2mm length, and fabric with zigzag stitches of a length of 2mm and a width of 5mm. (c) The stress-strain graph shows the impact of varying the properties of zigzag stitches. (d) An image of a sample with 1x5mm zigzag stitches shows the condition of the sample before uniaxial tensile loading. (e) An image of a sample with 1x5mm zigzag stitches shows the condition of the sample after uniaxial tensile loading. Notably, the fabric has failed while the sewn thread is intact.

During uniaxial tensile testing, it was revealed that stitch length and width are both critical factors that influence the tensile behavior of the samples with zigzag stitches. Figure 2 (c) shows stress-strain curves for samples with zigzag stitches of varying length and width. The fabric samples with 2x5mm, 2x4mm, and 3x5mm zigzag stitches failed at a higher strain than those with straight stitches but at a similar stress. As with the 2x5mm sample, the 2x4mm and 3x5mm had similar strain energy densities at low strain until the thread became a dominant influence. The 1x5mm zigzag sample exhibited drastically



different behavior from the other samples with zigzag stitches. The strain energy density of the 1x5mm zigzag samples matched that of the unaltered fabric sample up to approximately 60% strain, indicating that the stitches had little impact on the tensile behavior of the sample overall. The 1x5mm samples also had more extended elongation at failure than the unaltered fabric sample. The structure of the zigzag stitch contributes to the behavior of all the zigzag samples. Since zigzag stitches have both a stitch length and a stitch width, the stitch could change shape as the fabric elongates.

Figures 2(d) and (e) show a 1x5mm zigzag sample before and after uniaxial tensile testing. After testing, the stitches are longer in the direction parallel to loading and shorter in the direction perpendicular to loading compared to before tensile testing. In other words, the stitch could shrink in the direction perpendicular to loading while elongating in the direction of loading. A shorter stitch length results in more threads in the sample, which allows the stitches to deform enough to match the elongation of the fabric. The consequence of the stitch deformation is that the fabric withstands the load while the stitch can deform, but the stitch bears the load when it is no longer able to match the elongation of the fabric. Eventually, the load exhausts the ability of the stitch to deform, which is when the strain energy density of the zigzag sample deviates from that of the unaltered fabric. It was observed that the sewn thread had snapped in all samples after the sample had failed during tensile testing, except for the 1x5mm zigzag sample. The 1x5mm zigzag sample in Figure 2(c) had a shorter stitch length. Another point of interest is shown in Figure 2(e), which shows that the thread was intact after the fabric failed, which is the opposite of all other samples that contained sewn stitches. Therefore, it is possible to alter stitch properties to alter the fabric's tensile behavior, and the properties determine the extent of the influence from the thread and the fabric at particular strains.

### ***Repeated Cycling Behavior***

The unaltered fabric sample, straight stitch sample, and 2x5mm zigzag stitch sample were examined under cyclic loading to analyze stress softening and hysteresis. Any fabrics are subjected to cyclic loading during use from body movements such as the expansion of the chest during breathing or the movement of joints. An analysis of the behavior of the fabric samples during cyclic loading provides information that can inform design decisions. All samples were strained up to 10% because the straight stitch samples failed at approximately 12% strain. Hysteresis, the change in behavior from the loading to the unloading cycle, was observed in all samples, as shown in Figure 3. Across all samples, the most extensive hysteresis occurred during the first cycle. Additionally, all samples had the highest strain energy density during the loading of the first cycle. The hysteresis between the loading and unloading cycle of the overall sample is impacted by the relationship between the yarns' properties and the fabric's structure. The plastic deformation of the yarns, which relates to the slippage and viscoelasticity of the fibers within the yarn, influences hysteresis.<sup>10</sup> The structure dictates the number and nature of the contact points between loops of thread, which impacts the friction during loading. Friction is the main factor determining the amount of hysteresis that will occur.<sup>5</sup> In the samples with stitches, the causes of tensile hysteresis are further complicated by the presence the stitched threads, which impact the overall properties and structure of the

sample. In Figure 3b, the straight stitch sample showed more hysteresis than the zigzag stitched sample shown in Figure 3c, indicating that the straight stitched threads experienced more plastic deformation than the zigzag stitched threads. The difference in the plastic deformation experienced in the threads relates to the behavior observed in the uniaxial tensile testing. The straight-stitched thread sustains more of the load for the entire sample than the zigzag stitch; the thread in the straight-stitched sample experiences more plastic deformation. Repeated cycles allow for an investigation of the hysteresis in additional cycles and an analysis of the stress-softening behavior of the samples. The second cycle revealed that stress softening occurred in all samples between the first and second cycles, which can be observed in whole Figure 3 as a reduction in the strain energy density of the loading curve between the first and second cycles. The unaltered fabric sample in Figure 3a showed a minor stress softening, which can be attributed to the significant difference between the maximum strain during cyclic loading and the strain required to cause failure. Since the unaltered fabric sample has minor unrecoverable deformation at the 10% strain tested in this experiment, minimal stress softening occurred. In additional cycles after the second cycle, hysteresis in the fabric sample and the zigzag sample remained the same; however, hysteresis decreased slightly in the straight stitched sample from the second to the third cycle. The decrease in hysteresis is attributable to the stress softening in the straight stitch sample between the second and the third cycles, which indicates that further unrecoverable deformation occurred during each cycle. In comparison, the fabric and the zigzag stitch samples do not experience significant unrecoverable deformation in cycles after the second cycle.

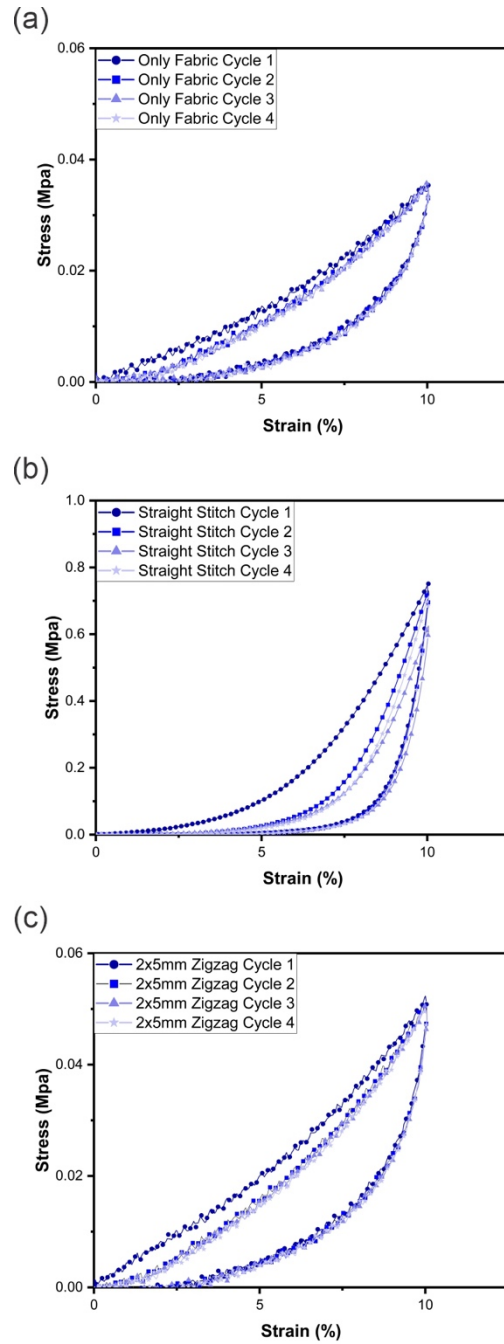


**Figure 2:** (a) The unaltered fabric sample showed less stress softening than the 2x5mm zigzag stitch sample but still showed hysteresis. (b) The straight stitch sample had the most stress softening and also showed hysteresis. (c) The cyclic loading of the 2x5mm zigzag stitch sample showed stress softening after the first cycle and hysteresis.

## ***Revealing rheological parameters of Fabric and Composite Systems***

The TNM is a powerful constitutive model capturing the flow and deformation (rheology) behaviors of materials. Bergstrom and Bischoff explained the mathematical details of the TNM in their work.<sup>1</sup> While the stress-strain analysis directly measures the mechanical behavior, the rheological parameters we often overlook in stress-strain analyses can be revealed through constitutive models. Studies on such parameters also enable data-informed design decisions.

We used MCalibration software to perform rheological analyses using TNM and calibrate the TNM parameters to assess unaltered and altered fabrics. MCalibration software begins calibration with a set of initially estimated parameter values by observing the experimental data. It tries to reduce the deviation between the predicted and the experimental behavior by continuously updating the parameters. This process is also known as data calibration and rheological parameter identification. When the coefficient of determination or the  $R^2$  value stops changing significantly by reaching convergence, the software reveals the rheological parameters in its user interface. The experimental data and MCalibration predicted data with their respective  $R^2$  fitness are shown in Figure 4, indicating that the TNM model effectively captures the uniaxial tensile behavior of unaltered, straight- and zigzag-stitched fabrics. The predicted data fits closely with the experimental data for all investigated samples with this method. The prediction of the 2x5mm zigzag sample in Figure 4a matched with an  $R^2$  fitness of 0.999, which was a closer fit than the unaltered fabric sample or the straight stitch sample. The reason for the closer match indicates that the 2x5mm zigzag sample had behavior closest to that of a thermoplastic polymer, which is the material on which the TNM is based. Furthermore, the calibration calculates the material model parameters, revealing information about the behavior of the samples that cannot be determined from an analysis of the experimental data alone. Table 1 shows several such parameters.

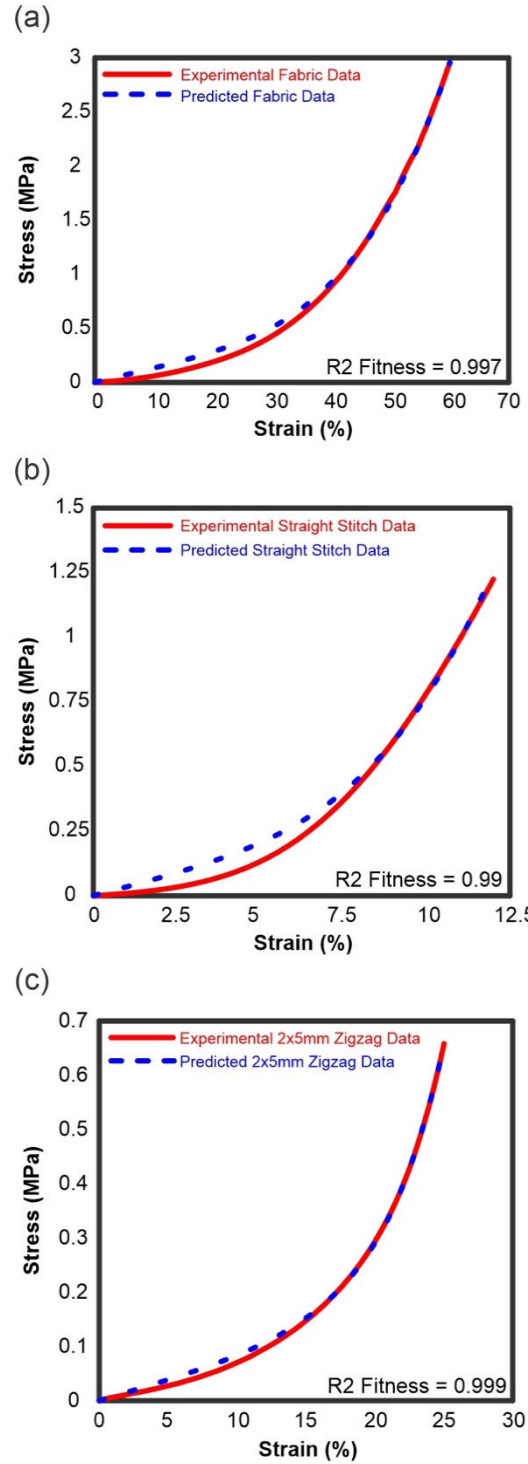


**Figure 3:** The material calibration with the PolyUMod TNM resulted in a good prediction for (a) the unaltered fabric sample, (b) the 2mm straight stitch sample, and (c) the 2x5mm zigzag sample.

**Table 1:** The Three-Network Model (TNM) parameters of unaltered fabric, straight stitch, and the 2x5 mm Zigzag stitch

Description	Symbol	Unit	Unaltered Fabric	Straight Stitch	2x5 mm Zigzag
Shear modulus of network A	$\mu_A$	KPa	11.40	77.95	0.65
Locking stretch	$\lambda_L$	-	1.08	1.02	1.04
Bulk modulus	$\kappa$	KPa	656.37	1369.34	1194.72
Flow resistance of network A	$\hat{\tau}_A$	KPa	127.80	901.91	352.31
Stress exponential of network A	$m_A$	-	3.83	11.11	9.59
Initial shear modulus of network B	$\mu_{Bi}$	KPa	96.46	15.05	40.75
Final shear modulus of network B	$\mu_{Bf}$	KPa	96.46	9.31	58.99
Evolution rate of $\mu_B$	$\beta$	-	9.69	10.20	10.50
Flow resistance of network B	$\hat{\tau}_B$	KPa	348.78	1226.80	636.76
Stress exponential of network B	$m_B$	-	7.89	9.65	10.85
Shear modulus of network C	$\mu_C$	KPa	398.95	1180.98	207.47

Earlier investigation<sup>27</sup> on assessing the hyperelastic material model calibrated parameters, leveraging Mooney-Rivlin, Ogden, neo-Hookean, Arruda Boyce, Gent, Yeoh, and Blatz-Ko constitutive models. The higher-order Mooney-Rivlin and Yeoh models fitted the experimental data properly. The Arruda-Boyce model also showed good relation with the experimental data. Also, we noticed a similarity in the stress-strain behavior from that investigation that is close to our unaltered fabric behavior shown in Figure 2(b). We want to compare the parameters we obtained with that literature<sup>27</sup>. We noted a shear modulus of 3.8913 KPa, and a limiting locking stretch ( $\lambda_{L,lim}$ ) of 0.65907 from that investigation. The Cauchy stress acting on any networks in the TNM model is based on the Arruda-Boyce or eight-chain model.<sup>1</sup> The reported shear modulus and the shear modulus of the Network A of the unaltered fabric are also not significantly different here. As the shear modulus of the Arruda-Boyce model gets distributed in three networks, we should only compare the locking stretch directly. The locking stretch is defined as the ratio of the current chain length and the initial chain length. From the literature, the relation between the locking stretch ( $\lambda_L$ ) and limited locking stretch can be found,<sup>34,35</sup> which is

$$\lambda_L = \sqrt{\frac{1}{3} \left( \lambda_{L,lim}^2 + \frac{2}{\lambda_{L,lim}} \right)}$$

The reported limiting locking stretch converted to  $\lambda_L$  will be 1.0753, which is very close to our reported locking stretch value of the unaltered fabric, 1.08. Additionally, for all the samples, the locking stretch was close to 1, indicating that the sample did not go through a significant strain level. The locking stretch values of the straight stitch and the zigzag stitch are also smaller than the unaltered fabric, indicating less deformation observed in Figure 2(b). The final calibrated parameters depend significantly on the initially guessed parameters. It would be easier to compare the parameters between three samples if an identical set of initial values was used. As we are using the uniaxial tensile testing here, bulk modulus should not impact the predicted behavior significantly.<sup>36</sup> In the TNM, network A and B utilize separate energy activation mechanisms to represent the amorphous and semi-crystalline domains. Network C represents the large strain response controlled by entropic resistance. The shear modulus and the flow resistance of network A in the straight stitch are significantly higher than the other two samples indicating higher resistance by the spring represented in the network. Figure 4(b) also indicates that up to 10% strain straight-stitched fabric is stiffer than the other two matching the observation in the parameters. Comparatively close initial and final shear modulus of network B and almost similar evolution rates indicate a similar effective shear modulus for all the samples. The flow resistance of network B and the shear modulus of network C of the straight-stitched sample are also higher, indicating higher stiffness of the materials.

## Conclusion

This work determined that altering the parameters of the stitching when sewing with cotton thread into a single layer of jersey-knit cotton fabric impacts the strain-energy density, hysteresis, and stress softening of the sample. When examined with optical and scanning electron microscopes, the stitched samples did not show damage to the fabric from the sewing process. The stitch type and parameters of a zigzag stitch were shown to directly impact the sample's behavior under uniaxial tensile loading. Depending on the stitch type, the fabric can be altered to have a higher or lower strain energy density at certain strains. We also note that stitches capable of less elongation than the fabric will increase the strain energy density at lower strains and result in failure at a lower strain. Stitches that can match or exceed the elongation may have minimal impact on the strain energy density of the sample at the same strains as a sample without stitches but will fail at higher strains, resulting in a higher strain energy density at failure. Stitches will also impact the hysteresis and stress softening of the sample. Also, stitches capable of less elongation than the fabric will be subjected to higher stress during loading, resulting in plastic deformation and more significant hysteresis and stress softening during cyclic loading. The tensile and cyclic tests reveal that the mechanical behavior of samples composed of fabric with stitches varies greatly depending on the relationships between the property of the materials and their structure. When data from tensile tests were calibrated with the PolyUMod TNM, the materials presented in this work matched well with the calibrated model; therefore, materials calibration provides an opportunity to aid the selection of materials and structure by offering insight into hidden parameters that allow for a data-driven approach to design.

Limitations of this work include the number of materials and structures investigated, as the behavior observed may differ from samples with different compositions and structures. Furthermore, many other properties may be impacted by the presence of sewing stitches that were not investigated in this paper, such as abrasive strength, bursting strength, torsional properties, ability to withstand washing and drying, and many other characteristics. Future works may investigate the impact of additional types of stitches on fabrics of different materials and structures and analyze additional properties of the samples.

## Acknowledgments

MRK acknowledges the funding support from VPRI's startup account. HW acknowledges the Nevada undergraduate research award (NURA) fund from the Undergraduate Research Office, and KZH acknowledges funding from the College of Engineering Dean's Office at the University of Nevada, Reno. HW acknowledges contributions from Sydney Fields, Jake Kattelman, Thomas Kaps, and Braden Norris for the MSE 470 (Polymer Engineering instructed by MRK) in-class project. KZH acknowledges the opportunity to train and mentor all the groups in CHE/MSE 470 and Brian Perdue in CHE 495 using the concepts from this article. MRK acknowledges the support received from Dean's Office to purchase Instron 5982 with Dr. Jefferey Lacombe, Dr. Bin Li, and Zachary Karmioli.

## References

1. Bergstrom JS, Bischoff JE. An Advanced Thermomechanical Constitutive Model for UHMWPE. *Int J Struct Chang Solids* 2010; 2: 31–39.
2. PolyUMod Three Network (TN) Model. *PolymerFEM.com*, <https://polymerfem.com/three-network-model/> (2020, accessed 21 February 2022).
3. Penava Ž, Penava DŠ, Miloš L. Experimental and analytical analyses of the knitted fabric off-axes tensile test. *Text Res J* 2021; 91: 62–72.
4. Mohamed A, Messiry ME. Analysis Of The Effect Of Cyclic Loading On Cotton-Spandex Knitted Fabric. pp. 1–6.
5. Dusserre G. Modelling the hysteretic wale-wise stretching behaviour of technical plain knits. *Eur J Mech - ASolids* 2015; 51: 160–171.
6. Li Q, Wang Y, Jiang S, et al. Investigation into tensile hysteresis of polyurethane-containing textile substrates for coated strain sensors. *Mater Des* 2020; 188: 108451.



7. Andrews BAK, McSherry WF, Frick JG, et al. Recovery from Tensile Strain in Knitted Cotton Fabric after Cross-Linking. *Text Res J* 1971; 41: 387–391.
8. Choi M-S, Ashdown SP. Effect of Changes in Knit Structure and Density on the Mechanical and Hand Properties of Weft-Knitted Fabrics for Outerwear. *Text Res J* 2000; 70: 1033–1045.
9. Liu R, Lao TT, Wang SX. Impact of Weft Laid-in Structural Knitting Design on Fabric Tension Behavior and Interfacial Pressure Performance of Circular Knits. *J Eng Fibers Fabr* 2013; 8: 155892501300800420.
10. Abdessalem SB, Abdelkader YB, Mokhtar S, et al. Influence of Elastane Consumption on Plated Plain Knitted Fabric Characteristics. *J Eng Fibers Fabr* 2009; 4: 155892500900400420.
11. Midha VK, Mukhopadhyay A, Chatopadhyay R, et al. Studies on the Changes in Tensile Properties of Sewing Thread at Different Sewing Stages. *Text Res J* 2009; 79: 1155–1167.
12. Midha VK, Mukhopadhyay A, Chattopadhyay R, et al. Effect of Process and Machine Parameters on Changes in Tensile Properties of Threads during High-speed Industrial Sewing. *Text Res J* 2010; 80: 491–507.
13. Sundaresan G, Salhotra KR, Hari PK. Strength reduction in sewing threads during high speed sewing in industrial lockstitch machine: Part II: Effect of thread and fabric properties. *Int J Cloth Sci Technol* 1998; 10: 64–79.
14. Sundaresan G, Hari PK, Salhotra KR. Strength reduction of sewing threads during high speed sewing in an industrial lockstitch machine: Part I - mechanism of thread strength reduction. *Int J Cloth Sci Technol* 1997; 9: 334–345.
15. Rengasamy RS, Wesley S. Tensile Behavior of Different Types of Sewing Threads Observed under Simple-Tensile, Loop and Knot Tests. *J Text Appar Technol Manag*; 7, <https://ojs.cnr.ncsu.edu/index.php/JTATM/article/view/1390> (2011, accessed 9 September 2022).
16. Abrishami S, Ezazshahabi N, Mousazadegan F. Analysis of the stress relaxation behaviour of sewing threads in the straight and loop form. *J Text Inst* 2021; 112: 596–609.
17. Villanueva R, Ganta D, Guzman C. Mechanical, in-situ electrical and thermal properties of wearable conductive textile yarn coated with polypyrrole/carbon black composite. *Mater Res Express* 2018; 6: 016307.
18. Ardalan S, Hosseinifard M, Vosough M, et al. Towards smart personalized perspiration analysis: An IoT-integrated cellulose-based microfluidic wearable patch

for smartphone fluorimetric multi-sensing of sweat biomarkers. *Biosens Bioelectron* 2020; 168: 112450.

19. Ukponmwan JO, Mukhopadhyay A, Chatterjee KN. Sewing Threads. *Text Prog* 2000; 30: 1–91.
20. Yıldız EZ, Pamuk O. The parameters affecting seam quality: a comprehensive review. *Res J Text Appar* 2021; 25: 309–329.
21. Sölar V, Meşegöl C, Kefsiz H, et al. A comparative study on seam performance of cotton and polyester woven fabrics. *J Text Inst* 2015; 106: 19–30.
22. Rogina-Car B, Schwarz I, Kovačević S. Analysis of Woven Fabric at the Place of the Sewn Seam. *AUTEX Res J* 2018; 18: 216–220.
23. Akter M, Khan MR. The effect of stitch types and sewing thread types on seam strength for cotton apparel. *Int J Sci Eng Res*; 6.
24. Wang L, Chan LK, Hu X. INFLUENCE OF STITCH DENSITY TO STITCHES PROPERTIES OF KNITTED PRODUCTS. *Res J Text Appar* 2001; 5: 46–53.
25. Admassu Y, Edae A, Getahun G, et al. Experimental analysis on the effect of fabric structures and seam performance characteristics of weft knitted cotton apparels. *J Eng Fibers Fabr* 2022; 17: 15589250221113480.
26. Qi HJ, Boyce MC. Constitutive model for stretch-induced softening of the stress–stretch behavior of elastomeric materials. *J Mech Phys Solids* 2004; 52: 2187–2205.
27. Julio García Ruíz M, Yarime Suárez González L. Comparison of hyperelastic material models in the analysis of fabrics. *Int J Cloth Sci Technol* 2006; 18: 314–325.
28. Khiêm VN, Krieger H, Itskov M, et al. An averaging based hyperelastic modeling and experimental analysis of non-crimp fabrics. *Int J Solids Struct* 2018; 154: 43–54.
29. Gong Y, Peng X, Yao Y, et al. An anisotropic hyperelastic constitutive model for thermoplastic woven composite preregs. *Compos Sci Technol* 2016; 128: 17–24.
30. Peng X, Guo Z, Du T, et al. A simple anisotropic hyperelastic constitutive model for textile fabrics with application to forming simulation. *Compos Part B Eng* 2013; 52: 275–281.
31. Peng XQ, Guo ZY, Zia-Ur-Rehman, et al. A Simple Anisotropic Fiber Reinforced Hyperelastic Constitutive Model for Woven Composite Fabrics. *Int J Mater Form* 2010; 3: 723–726.

32. MCalibration. *PolymerFEM.com*, <https://polymerfem.com/mcalibration/> (accessed 21 February 2022).
33. Geršak J, Knez B. REDUCTION IN THREAD STRENGTH AS A CAUSE OF LOADING IN THE SEWING PROCESS. *Int J Cloth Sci Technol* 1991; 3: 6–12.
34. Bergstrom JS. *Mechanics of Solid Polymers: Theory and Computational Modeling*. William Andrew, 2015.
35. Nguyen H-D, Huang S-C. The Uniaxial Stress–Strain Relationship of Hyperelastic Material Models of Rubber Cracks in the Platens of Papermaking Machines Based on Nonlinear Strain and Stress Measurements with the Finite Element Method. *Materials* 2021; 14: 7534.
36. Jorgen. How Important is the Bulk Modulus in FEA? *PolymerFEM.com*, <https://polymerfem.com/how-important-is-the-bulk-modulus/> (2021, accessed 17 November 2022).